

# Ranid Herpesvirus 3 Infection in Common Frog *Rana temporaria* Tadpoles

Francesco C. Origgi, Annette Taugbøl

Ranid herpesvirus 3 (RaHV3) is a recently discovered virus associated with skin disease in frogs. We detected RaHV3 DNA in free-ranging common frog (*Rana temporaria*) tadpoles, consistent with premetamorphic infection. Our finding reveals a critical aspect of RaHV3 pathogenesis, relevant for amphibian ecology and conservation and, potentially, for human health.

Infectious diseases have been identified as relevant stressors contributing to the ongoing global amphibian decline (1). The collapse of amphibian communities translates into a dramatic loss of biodiversity and critical biomass, which eventually could affect human health (2). Ranaviruses and chytrid fungi are primary amphibian pathogens that are causing extinction or extirpation of local amphibian populations worldwide (3,4). It is likely that other infectious organisms, yet to be characterized, might play a similar role.

Recently, 2 novel alloherpesviruses have been discovered: ranid herpesvirus 3 (RaHV3, *Batravirus ranidallo3*) in the common frog (*Rana temporaria*) and bufonid herpesvirus 1 in the common toad (*Bufo bufo*). Both viruses are associated with proliferative skin disease (5–7). RaHV3 is invariably associated with gray patchy skin proliferations corresponding to areas of epidermal hyperplasia (Figure 1) (7). Lesions vary in severity and size, but their clinical significance in adult frogs is unknown. Equally unclear is the potential effect of the lesions on overall host fitness, reproductive success, and susceptibility to other infectious agents.

Pathogenesis of RaHV3 is only partially understood (7); the actual route and timing of infection is

unknown. In a transmission study performed on post-metamorphic common frogs, no specific lesions could be observed after RaHV3 inoculation (F.C. Origgi, unpub. data). Furthermore, experimental transmission studies of ranid herpesvirus 1 (RaHV1, *Batravirus ranidallo1*), the first characterized amphibian herpesvirus (8), indicated that the virus-associated renal adenocarcinoma most likely occurred when amphibians were infected during the early embryonic stage (pre-metamorphosis), but not in adult or juvenile stages (postmetamorphosis) (as reviewed in 9). We investigated the potential occurrence of RaHV3 infection in premetamorphic free-ranging common frogs.

## The Study

We collected 14 sample batches of free-ranging tadpoles (3–13 tadpoles per batch), either directly from or in close (<10 m) proximity to 5 ponds in Norway in 2022, where adult frogs with lesions consistent with RaHV3 infection were observed earlier in the year (Figure 2) (F.C. Origgi, unpub. data). We sampled the ponds 2–3 times during early June through mid-July 2022 (Appendix Table, <https://wwwnc.cdc.gov/EID/article/29/6/23-0255-App1.pdf>). The Gosner developmental stages for tadpoles ranged from stages 26–36.

We collected and humanely euthanized tadpoles by using tricaine methanesulfonate in strict accordance with the Animal Welfare Act (§4 in FOR-2003-03-14-349) of Norway and then preserved them in 96% ethanol. In the laboratory, we bisected each tadpole with a scalpel; we extracted DNA from 1 half as previously described (5) and fixed the other half in 10% buffered formalin. We amplified the partial RaHV3 genome sequence as previously described (5) and by using a new quantitative PCR protocol (Appendix). Initially, we extracted DNA from 3–5 tadpoles from each sampling date and pond location; if we obtained a positive signal for RaHV3 by

---

Authors affiliations: University of Messina, Messina, Italy (F.C. Origgi); University of Bern, Bern, Switzerland (F.C. Origgi); Norwegian Institute for Nature Research, Lillehammer, Norway (A. Taugbøl)

DOI: <https://doi.org/10.3201/eid2906.230255>

PCR, we tested all tadpoles collected from the same location. We processed the fixed-tissues, embedded them in paraffin, prepared 5  $\mu\text{m}$ -thick sections, and stained the sections with hematoxylin and eosin in accordance with the standard protocol used at the Vetsuisse Faculty, University of Bern.

After qualitative and quantitative PCR on tadpole DNA ( $n = 77$  samples), we found 2 of 14 sampled batches were positive for RaHV3, corresponding to 2 of the 5 tested pond locations (Lillehammer and Skytta) (Figure 2). After testing each tadpole in the positive batches, we identified 6 of 13 tadpoles from the Lillehammer pond and 1 of 4 from the Skytta pond that were positive for RaHV3 DNA; genome equivalents ranged from  $2 \times 10^1$  to  $2 \times 10^7$ . After sequencing amplicons obtained by using qualitative PCR (5), we found a 100% match with the reference strain RaHV3\_FO1\_2015 (Genbank accession no. NC\_034618.1).

We did not observe differences in histological sections of RaHV3 PCR-positive and PCR-negative tadpoles. However, RaHV3-associated changes might have been masked by the advanced autolysis observed in the examined tissue sections.

## Conclusions

Finding genomic RaHV3 DNA in free-ranging tadpoles is a major step toward understanding the



**Figure 1.** Ranid herpesvirus 3 infection in common frog *Rana temporaria* tadpoles, Norway. Image shows a large number of multifocal to coalescent, mildly elevated, gray patches (epidermal hyperplasia) extending over most of the integument, particularly clustering along the left flank. Between gray areas is normally pigmented skin. Image copyright © Jeroen van der Kooij.

pathogenesis of RaHV3-associated disease. In particular, this result supports the hypothesis that infection occurs during the frog's premetamorphic embryonic or larval stages. Experimental RaHV1 infection of leopard frogs (*Lithobates pipiens*) was successful only

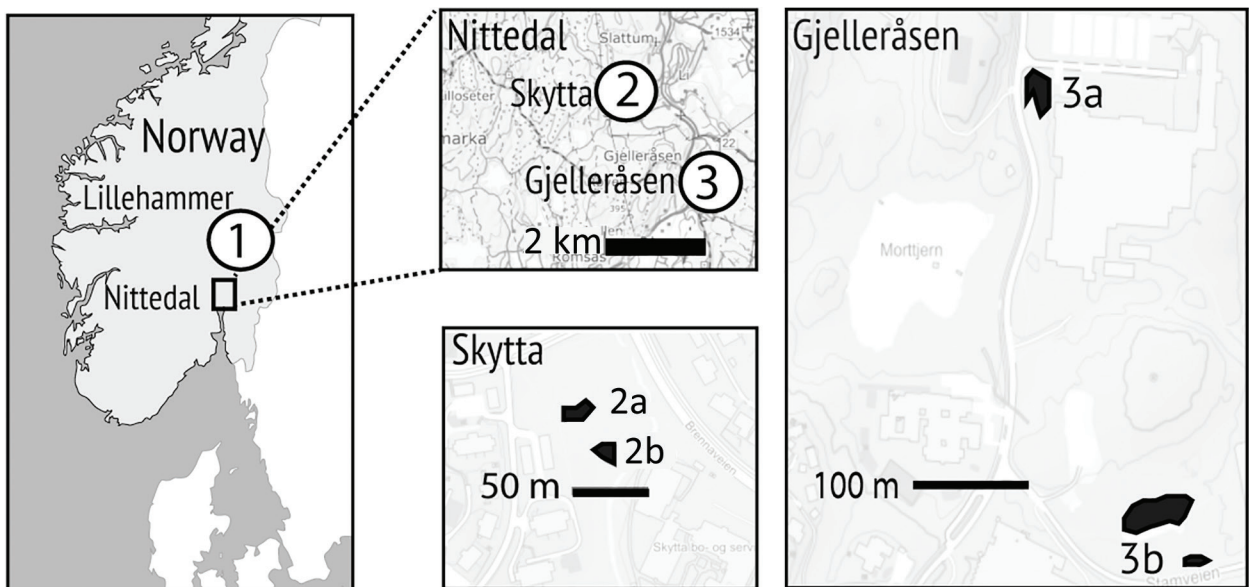


**Figure 2.** Location of sampling areas in study of ranid herpesvirus 3 infection in common frog *Rana temporaria* tadpoles, Norway. We collected 14 sample batches of free-ranging tadpoles (3–13 tadpoles per batch) either directly from or in close (<10 m) proximity to 5 ponds in Norway in 2022, where adult frogs with lesions consistent with ranid herpesvirus 3 (RaHV3) infection were observed earlier in the year. Maps show locations of ponds in Lillehammer, Skytta, and Gjelleråsen and the distances (in meters) between them. The 2 ponds marked collectively as 3b are linked by marshland in which adult frogs breed independently and are, therefore, treated as 1 complex. We found 2 of 14 sampled tadpole batches were positive for RaHV3 by using PCR, corresponding to pond areas in Lillehammer and Skytta. After testing each tadpole in the positive batches, we identified 6 of 13 tadpoles from the Lillehammer pond and 1 of 4 from the Skytta pond that were RaHV3-positive.

during the early embryonic stages (9). Why premetamorphic frogs are presumptively more susceptible to herpesvirus infections is unclear. The lack of keratinized skin in tadpoles (10) and the substantial immune system differences between premetamorphic and postmetamorphic life stages might partially explain the susceptibility of premetamorphic frogs to natural infection (11). Studies performed with RaHV1 did not clarify the natural route of infection because the embryos were experimentally inoculated with the virus in the pronephros, which is unlikely to mimic what occurs in nature (9). RaHV3-infected adult frogs are known to release a large number of virions embedded in sloughed keratinocytes (5,7), which could eventually be ingested by tadpoles. However, the possibility that oral ingestion of RaHV3 would cause tadpole infection, similarly to what has been shown for Ranavirus, a major amphibian pathogen (12), will need to be ruled out by a transmission study.

All 5 tadpole populations were collected in or near ponds where infected adults had been confirmed earlier in the Spring, but only 2 tadpole populations were RaHV3-positive and only at 1 timepoint for each pond (2 of 14 samples in total). Among the positive samples, the Lillehammer population had ≈50% and the Skytta population had ≈25% positivity rates. Reasons for discrepancies in incidence of RaHV3 infection between the different sampled populations remain unclear. Our finding suggests either sporadic RaHV3 infection within different tadpole populations, high virus lethality in infected tadpoles, or both. According to the second hypothesis, RaHV3-positive tadpoles would be difficult to detect in field conditions, because they would rapidly die and be scavenged. Herpesviruses, including alloherpesviruses, infecting a variety of animal species generally cause more severe disease and death in young, immature individuals than in adult hosts, (13). Accordingly, RaHV3 might be fatal to a large proportion of infected tadpoles resulting in low detection rates in the remaining viable tadpole population. No obvious tadpole die-offs had been recently reported at the sampling sites; however, those sites are not presently monitored.

In conclusion, our study opens a new venue for understanding RaHV3 pathogenesis and potential effects of RaHV3 infections on premetamorphic and postmetamorphic life stages of amphibian hosts. Understanding the short- and long-term consequences of RaHV3 and other herpesvirus infections on frog populations will be critical for amphibian conservation programs, maintaining biodiversity, and, in turn, supporting human and planetary health (2).

## Acknowledgments

We thank the technical personnel at Vetsuisse Bern, Institute of Animal Pathology, for histological analysis and Ian Hawkins for critical review of this manuscript.

Fieldwork was funded by the Norwegian Financial Mechanism 2014–2021, project no. 2019/34/H/NZ8/00683 (ECOPOND project). Development of molecular tests was partially supported by the Vontobel Foundation (Zurich, Switzerland) and Swiss Federal Office of the Environment (FOEN; grant no. R212-1468).

## About the Author

Dr. Origgi is a veterinary microbiologist and pathologist at the University of Messina and University of Bern. His research interests focus on infectious diseases and pathology of wildlife, especially reptiles and amphibians. Dr. Taugbøl is an evolutionary geneticist at the Norwegian Institute for Nature Research. Her research interests include biodiversity conservation.

## References

1. Catenazzi A. State of the world's amphibians. *Annu Rev Environ Resour.* 2015;40:91–119. <https://doi.org/10.1146/annurev-environ-102014-021358>
2. Springborn MR, Weill JA, Lips KR, Ibáñez R, Ghosh A. Amphibian collapses increased malaria incidence in Central America. *Environ Res Lett.* 2022;17:104012. <https://doi.org/10.1088/1748-9326/ac8e1d>
3. Price SJ, Garner TWJ, Nichols RA, Balloux F, Ayres C, Mora-Cabello de Alba A, et al. Collapse of amphibian communities due to an introduced *Ranavirus*. *Curr Biol.* 2014;24:2586–91. <https://doi.org/10.1016/j.cub.2014.09.028>
4. Skerratt LF, Berger L, Speare R, Cashins S, McDonald KR, Phillott AD, et al. Spread of chytridiomycosis has caused the rapid global decline and extinction of frogs. *EcoHealth.* 2007;4:125–34. <https://doi.org/10.1007/s10393-007-0093-5>
5. Origgi FC, Schmidt BR, Lohmann P, Otten P, Akdesir E, Gaschen V, et al. Rapid herpesvirus 3 and proliferative dermatitis in free-ranging wild common frogs (*Rana temporaria*). *Vet Pathol.* 2017;54:686–94. <https://doi.org/10.1177/0300985817705176>
6. Origgi FC, Schmidt BR, Lohmann P, Otten P, Meier RK, Pisano SRR, et al. Bufonid herpesvirus 1 (BfHV1) associated dermatitis and mortality in free ranging common toads (*Bufo bufo*) in Switzerland. *Sci Rep.* 2018;8:14737. <https://doi.org/10.1038/s41598-018-32841-0>
7. Origgi FC, Otten P, Lohmann P, Sattler U, Wahli T, Lavazza A, et al. Herpesvirus-associated proliferative skin disease in frogs and toads: proposed pathogenesis. *Vet Pathol.* 2021;58:713–29. <https://doi.org/10.1177/03009858211006385>
8. Lucké B. A neoplastic disease of the kidney of the frog, *Rana pipiens*. *Am J Cancer.* 1934;20:352–79. <https://doi.org/10.1158/ajc.1934.352>
9. McKinnell RG. The Lucké frog kidney tumor and its herpesvirus. *Am Zool.* 1973;13:97–114. <https://doi.org/10.1093/icb/13.1.97>
10. Marantelli G, Berger L, Speare R, Keegan L. Distribution of the amphibian chytrid *Batrachochytrium dendrobatidis* and

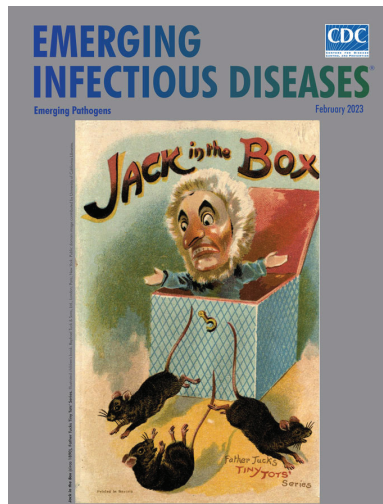


- keratin during tadpole development. *Pac Conserv Biol.* 2004;10:173–9. <https://doi.org/10.1071/PC040173>
11. Rollins-Smith LA, Blair PJ, Davis AT. Thymus ontogeny in frogs: T-cell renewal at metamorphosis. *Dev Immunol.* 1992;2:207–13. <https://doi.org/10.1155/1992/26251>
  12. Hoverman JT, Gray MJ, Miller DL. Anuran susceptibilities to ranaviruses: role of species identity, exposure route, and a novel virus isolate. *Dis Aquat Organ.* 2010;89:97–107. <https://doi.org/10.3354/dao02200>
  13. Michel B, Fournier G, Loeffrig F, Costes B, Vanderplasschen A. Cyprinid herpesvirus 3. *Emerg Infect Dis.* 2010;16:1835–43. <https://doi.org/10.3201/eid1612.100593>
- Address for correspondence: Francesco Origgi, Institute of Infectious Animal Diseases, Department of Veterinary Sciences, University of Messina, Viale Giovanni Palatucci sn, 98168 Messina, Italy; email: foriggi@unime.it; or Institute of Animal Pathology, Vetsuisse Faculty, University of Bern, Länggassstrasse 122, CH-3012, Bern, Switzerland; email: francesco.origgi@vetsuisse.unibe.ch

February 2023

## Emerging Pathogens

- Infant Botulism, Israel, 2007–2021
- Sentinel Surveillance System Implementation and Evaluation for SARS-CoV-2 Genomic Data, Washington, USA, 2020–2021
- Crimean-Congo Hemorrhagic Fever, Spain, 2013–2021
- *Streptococcus dysgalactiae* Bloodstream Infections, Norway, 1999–2021
- Relationship between Telework Experience and Presenteeism during COVID-19 Pandemic, United States, March–November 2020
- Circovirus Hepatitis Infection in Heart-Lung Transplant Patient, France
- Incidence and Transmission Dynamics of *Bordetella pertussis* Infection in Rural and Urban Communities, South Africa, 2016–2018
- Influence of Landscape Patterns on Exposure to Lassa Fever Virus, Guinea
- Increased Multidrug-Resistant *Salmonella enterica* I Serotype 4,[5],12:i:- Infections Associated with Pork, United States, 2009–2018
- Novel Prion Strain as Cause of Chronic Wasting Disease in a Moose, Finland
- Novel Species of *Brucella* Causing Human Brucellosis, French Guiana
- Penicillin and Cefotaxime Resistance of Quinolone-Resistant *Neisseria meningitidis* Clonal Complex 4821, Shanghai, China, 1965–2020
- Combined Phylogeographic Analyses and Epidemiologic Contact Tracing to Characterize Atypically Pathogenic Avian Influenza (H3N1) Epidemic, Belgium, 2019



- (Mis)perception and Use of Unsterile Water in Home Medical Devices, PN View 360+ Survey, United States, August 2021
- Molecular Detection of *Candidatus Orientia chuto* in Wildlife, Saudi Arabia
- Neohrlchiosis in Symptomatic Immunocompetent Child, South Africa
- Successful Drug-Mediated Host Clearance of *Batrachochytrium salamandrivorans*
- Powassan Virus Lineage I in Field-Collected *Dermacentor variabilis* Ticks, New York, USA
- *Bartonella* spp. and Typhus Group Rickettsiae among Persons Experiencing Homelessness, São Paulo, Brazil
- Changing Disease Course of Crimean-Congo Hemorrhagic Fever in Children, Turkey
- Estimated Cases Averted by COVID-19 Digital Exposure Notification, Pennsylvania, USA, November 8, 2020–January 2, 2021
- Next-Generation Sequencing for Identifying Unknown Pathogens in Sentinel Immunocompromised Hosts
- Orthopoxvirus Infections in Rodents, Nigeria, 2018–2019
- Occupational Monkeypox Virus Transmission to Healthcare Worker, California, USA, 2022
- Familial Monkeypox Virus Infection Involving 2 Young Children
- *Dirofilaria immitis* in Dog Imported from Venezuela to Chile
- Relapsing Fever Caused by *Borrelia lonestari* after Tick Bite in Alabama, USA
- Age-Stratified Model to Assess Health Outcomes of COVID-19 Vaccination Strategies, Ghana
- Early Introduction and Community Transmission of SARS-CoV-2 Omicron Variant, New York, New York, USA
- Correlates of Protection, Thresholds of Protection, and Immunobridging among Persons with SARS-CoV-2 Infection
- Longitudinal Analysis of Electronic Health Information to Identify Possible COVID-19 Sequelae
- Nipah Virus Exposure in Domestic and Peridomestic Animals Living in Human Outbreak Sites, Bangladesh, 2013–2015
- *Candida auris* Discovery through Community Wastewater Surveillance during Healthcare Outbreak, Nevada, USA, 2022

**EMERGING  
INFECTIOUS DISEASES®**

To revisit the February 2023 issue, go to:  
<https://wwwnc.cdc.gov/eid/articles/issue/29/2/table-of-contents>

*EID cannot ensure accessibility for supplementary materials supplied by authors. Readers who have difficulty accessing supplementary content should contact the authors for assistance.*

# Ranid Herpesvirus 3 Infection in Common Frog *Rana temporaria* Tadpoles, Norway

## Appendix

### Additional Methods

#### Quantitative PCR Primer and Probe Design

A forward (FW-5'-GCAGGACACAATTCAAGCGG-3') and reverse (RV-5'-TTTACTGCGGTATAGCGCCC-3') primer set and minor groove binder probe (5'-FAM-TGGCGAACAGTGTCAACAGT-3') were designed in silico by using Geneious 10.0 software (<https://www.geneious.com>). We used the DNA polymerase gene of ranid herpesvirus 3 (RaHV3, *Batravirus ranidallo3*) (1), a highly conserved gene among the order Herpesvirales, as the DNA template. The amplified amplicon was predicted to be 105 nt.

#### Positive PCR Control Synthesis

The positive control consisting of DNA amplified by the selected primers was obtained by qualitative PCR. In brief, the master mix contained 3.75  $\mu$ L 25 mM MgCl<sub>2</sub> solution, 3  $\mu$ L 10 $\times$  buffer, 0.4  $\mu$ L 10 mM dNTP mix, 0.2  $\mu$ L Firepol DNA polymerase (Solis BioDyne, <https://www.solisbiodyne.com>), 100 ng of DNA (total DNA from an RaHV3 naturally infected frog) (1), and double distilled H<sub>2</sub>O (ddH<sub>2</sub>O) for a total of 30  $\mu$ L. PCR included a denaturing step at 94°C for 3 min; then 40 cycles comprising 30 s at 94°C (denaturing step), 30 s at 55°C (annealing step), and 30 s at 72°C (extension step). A final 10 min extension step at 72°C was used to exhaust the polymerase. The samples were then resolved in a 2% agarose gel and examined under ultraviolet light.

The PCR amplicon was then cloned into the pGEM-T-Easy vector (Promega, <https://www.promega.com>) by following the manufacturer's instructions. Positive white colonies (blue/white selection) were screened, amplified, and the plasmid was purified by using an

established protocol (2). The identity of the amplicon was confirmed by automated Sanger sequencing (both strands) (Microsynth AG, <https://www.microsynth.com>). The sequenced amplicon matched 100% with the expected amplified partial sequence of the RaHV3 DNA polymerase gene and was 105 nt, as expected.

The molecular weight of the positive control DNA amplicon cloned into the expression vector and the corresponding number of molecules contained in 1 ng DNA were determined by using the following formula (<https://bitesizebio.com/20669/how-to-calculate-the-number-of-molecules-in-any-piece-of-dna>):

$$\text{number of copies} = \text{ng DNA} \times (6.022 \times 10^{23}) / \text{length} \times (1 \times 10^9) \times 650.$$

The amplicon was 105 bp and plasmid was 3015 bp, resulting in  $2.97 \times 10^8$  plasmid copies per ng plasmid DNA.

#### **Real-Time PCR Sensitivity Assay**

We prepared 10-fold dilutions of the target plasmid in ddH<sub>2</sub>O, ranging from  $10^6$  to  $10^{-2}$  copies/ $\mu$ L, and tested the diluted plasmids by using real-time PCR. Samples were tested in duplicate ( $10^6$  to  $10^2$  copies/ $\mu$ L), triplicate ( $10^1$  copies/ $\mu$ L), or quintuplicate ( $10^0$  copies/ $\mu$ L). The cycling conditions for real-time PCR were: a denaturation step at 95°C for 3 min, then 45 cycles of a denaturation step at 95°C for 30 s and annealing and extension step at 60°C for 1 min. The reactions were performed on an Applied Biosystems 7500 Fast cycler (Thermo Fisher Scientific, <https://www.thermofisher.com>). The PCR mix consisted of 10  $\mu$ L 2 $\times$  qPCR Master Mix (Thermo Fisher), 900 nmol/L of each primer, 250 nmol/L minor groove binder probe (Thermo Fisher), 100 ng of total DNA (for field samples; 1  $\mu$ L of plasmid suspension for titration), and ddH<sub>2</sub>O for a total of 20  $\mu$ L.

The quantitative PCR protocol enabled the detection of  $\geq 1$  copy of target plasmid per reaction (cycle threshold 39). The  $R^2$  value was 0.99, slope was  $-3.49$ , and y intercept was 38.71. The primer efficiency was 93.43% (<https://www.thermofisher.com/it/en/home/brands/thermo-scientific/molecular-biology/molecular-biology-learning-center/molecular-biology-resource-library/thermo-scientific-web-tools/qpcr-efficiency-calculator.html>).

## References

1. Origi FC, Schmidt BR, Lohmann P, Otten P, Akdesir E, Gaschen V, et al. Ranid herpesvirus 3 and proliferative dermatitis in free-ranging wild common frogs (*Rana temporaria*). *Vet Pathol.* 2017;54:686–94. [PubMed https://doi.org/10.1177/0300985817705176](https://doi.org/10.1177/0300985817705176)
2. Origi FC, Plattet P, Sattler U, Robert N, Casaubon J, Mavrot F, et al. Emergence of canine distemper virus strains with modified molecular signature and enhanced neuronal tropism leading to high mortality in wild carnivores. *Vet Pathol.* 2012;49:913–29. [PubMed https://doi.org/10.1177/0300985812436743](https://doi.org/10.1177/0300985812436743)

**Appendix Table.** Summary of collection dates, pond locations, and tadpole sample types.

Sample date	Pond location	Area code	Sample type
2022 Jun 4*	Lillehammer	1	Larvae
2022 Jun 16	Lillehammer	1	Larvae
2022 Jun 4	Skytta1	2a	Larvae
2022 Jun 26	Skytta1	2a	Larvae
2022 Jul 10	Skytta1	2a	Larvae
2022 Jun 4*	Skytta2	2b	Larvae
2022 Jun 26	Skytta2	2b	Larvae
2022 Jul 10	Skytta2	2b	Larvae
2022 Jun 4	Pryddammen	3a	Larvae
2022 Jun 26	Pryddammen	3a	Larvae
2022 Jul 10	Pryddammen	3a	Larvae
2022 Jun 4	Froskedammen	3b	Larvae
2022 Jun 26	Froskedammen	3b	Larvae
2022 Jul 10	Froskedammen	3b	Larvae

\*Dates and locations where tadpole sample batches were positive for ranid herpesvirus 3.